NEOPLASIA
www.neoplasia.com

Volume 11 Number 6 June 2009 pp. 529–541 **529**

Inflammatory Cytokine Tumor Necrosis Factor α Confers Precancerous Phenotype in an Organoid Model of Normal Human Ovarian Surface Epithelial Cells[1]

Joseph Kwong*,†,2, Franky Leung Chan‡, Kwong-kwok Wong§, Michael J. Birrer¶, Kyra M. Archibald†, Frances R. Balkwill†, Ross S. Berkowitz*,# and Samuel C. Mok*,#,3

*Laboratory of Gynecologic Oncology, Division of Gynecologic Oncology, Department of Obstetrics, Gynecology and Reproductive Biology, Brigham and Women's Hospital, Harvard Medical School, Boston, MA, USA; †Centre for Cancer and Inflammation, Institute of Cancer, Barts and The London School of Medicine and Dentistry, Queen Mary University of London, Charterhouse Square, London EC1M 6BQ, UK; ‡Department of Anatomy, The Chinese University of Hong Kong, Hong Kong, China; §Department of Gynecologic Oncology, University of Texas M.D. Anderson Cancer Center, Houston, TX, USA; ¶Cell and Cancer Biology Branch, National Cancer Institute, Bethesda, MD, USA; #Dana-Farber Harvard Cancer Center, Dana-Farber Cancer Institute, Harvard Medical School, Boston, MA, USA

Abstract

In this study, we established an *in vitro* organoid model of normal human ovarian surface epithelial (HOSE) cells. The spheroids of these normal HOSE cells resembled epithelial inclusion cysts in human ovarian cortex, which are the cells of origin of ovarian epithelial tumor. Because there are strong correlations between chronic inflammation and the incidence of ovarian cancer, we used the organoid model to test whether protumor inflammatory cytokine tumor necrosis factor α would induce malignant phenotype in normal HOSE cells. Prolonged treatment of tumor necrosis factor α induced phenotypic changes of the HOSE spheroids, which exhibited the characteristics of precancerous lesions of ovarian epithelial tumors, including reinitiation of cell proliferation, structural disorganization, epithelial stratification, loss of epithelial polarity, degradation of basement membrane, cell invasion, and overexpression of ovarian cancer markers. The result of this study provides not only an evidence supporting the link between chronic inflammation and ovarian cancer formation but also a relevant and novel *in vitro* model for studying of early events of ovarian cancer.

Neoplasia (2009) 11, 529–541

Address all correspondence to: Joseph Kwong, Department of Obstetrics and Gynaecology, The Chinese University of Hong Kong, Block E, 1/F, Prince of Wales Hospital, Shatin, Hong Kong, China. E-mail: josephkwong@cuhk.edu.hk

[1]This study was supported by The Ovarian Cancer Fund Inc (Research Training Program of Excellence Grant) and Association for International Cancer Research (AICR) to J.K.; R33CA103595 and The Ovarian Cancer SPORE P50CA165009 from National Institutes of Health, Department of Health and Human Service; The Gillette Center for Women's Cancer; Adler Foundation Inc.; The Morse Family Fund; and The Natalie Pihl Fund (to S.C.M. and R.S.B.); HEFCE for F.R.B.; Cancer Research UK Studentship for K.M.A.

[2]Present address: Department of Obstetrics and Gynaecology, The Chinese University of Hong Kong, Hong Kong, China.
[3]Present address: Department of Gynecologic Oncology, University of Texas M.D. Anderson Cancer Center, Houston, TX.

Received 5 January 2009; Revised 18 March 2009; Accepted 18 March 2009

DOI 10.1593/neo.09112

Introduction

Ovarian cancer is the most lethal gynecological cancer in the United States and Europe. A high mortality rate makes this disease a major women's health concern. Approximately 70% of patients whose conditions are diagnosed with ovarian cancer will present at advanced stages (FIGO stages III and IV), whereas the 5-year survival rate for this group of patients is only 10% to 40% [1]. Unclear etiology of ovarian cancer and incomplete understanding of the nature of its precursor lesions are the major reasons for the slow development of early detection markers and targeted therapy. In addition, lack of transgenic mouse models that recapitulate clinical features of early-stage ovarian cancer also makes study of early events of ovarian cancer difficult.

Although all cell types in the human ovary (including epithelial, stromal, and germ cells) may undergo tumor transformation, 80% to 90% of malignant ovarian tumors are originated from the single layer of epithelial cells covering the ovaries [2]. In addition to the surface epithelium of ovary, there are epithelial inclusion cysts that are simply cysts lined by a single layer of epithelium and located in the human ovarian cortex [3], which can be found in fetal and newborn ovaries [4] but more frequently in the ovaries of aged women [3,5]. Most importantly, the epithelial inclusion cysts have a greater propensity to tumor development than the surface epithelium of the ovary [5]. This may be due to the preferential location of the epithelial inclusion cysts that are exposed to tumor-promoting factors in the microenvironment of ovarian cortex [6].

In the past decade, epidemiological data suggested that chronic inflammation is associated with ovarian tumor development. Studies showed that factors relating to inflammation of the ovarian surface epithelium (OSE; such as asbestos and talc exposure, endometriosis, and pelvis inflammatory diseases) are associated with an increased risk for ovarian cancer [7–9]. Nevertheless, tubal ligation and hysterectomy were shown to be the protective factors against ovarian cancer because these procedures reduce the exposure of the OSE to inflammatory agents [7,10]. Latest statistics also showed that the use of aspirin or other nonsteroidal anti-inflammatory drugs reduces the risk of ovarian cancer [9,11].

Among inflammatory mediators, several cytokines (such as tumor necrosis factor α (TNF-α), interleukin 1β (IL-1β), and IL-6) produced by activated innate immune cells have been shown to promote tumor growth and progression [12]. The roles of cytokines in the development of ovarian cancer have also been investigated previously. Studies showed that TNF-α would particularly promote tumor progression, invasion, and metastasis of ovarian cancer cells [13–15]. However, the roles of TNF-α in tumor initiation in normal human ovarian surface epithelial (HOSE) cells remain largely unknown. Therefore, in this study, we have established an *in vitro* organoid model of normal HOSE cells, which mimics ovarian inclusion cysts, and used the model to test whether the inflammatory cytokine TNF-α would induce malignant phenotype in normal HOSE cells.

Materials and Methods

Reagents

Recombinant human TNF-α was purchased from Calbiochem (La Jolla, CA). Anti–Ki-67, anti-calretinin, and anti-CA125 antibodies were obtained from Zymed (South San Francisco, CA); anti–cleaved caspase 3 (Asp175) and anti–ezrin/radixin/moesin (ERM) were obtained from Cell Signaling Technology (Beverly, MA); anti–claudin 4, anti–heparan sulfate proteoglycan (HSPG), and anti–matrix metalloproteinase 10 (MMP-10) were obtained from Lab Vision Corporation (Fremont, CA); anti–cytokeratin AE1&3 and anti–Laminin V were obtained from Chemicon International (Temecula, CA); anti-GM130 and ECAD were from BD Transduction Laboratories (Franklin Lakes, NJ); anti–human collagen IV, anti–human epithelial membrane antigen (EMA/MUC1), anti–human epithelial antigen (EpCAM) were purchased from DakoCytomation (Carpinteria, CA).

Tissue Culture

Fragments of HOSE cells were detached with a SAFETEX sterile cytology brush (Andwin Scientific, Warner Center, CA) from the surface of grossly normal ovaries. The specimens were obtained with consent from patients having surgery for benign gynecologic diseases. The cells were cultured in Medium199/MCDB105 (Sigma, St. Louis, MO) with 15% FBS for 1 week, then maintained in complete medium with 10% FBS until confluent in a 25-cm^2 flask. Normal HOSE cells in the primary cultures were confirmed by their characteristic epithelial morphology and immunofluorescent staining of cytokeratin (AE1&3) and calretinin. First passages of primary cultures with more than 95% of normal HOSE cells were used. Human papilloma virus (HPV) E6/E7–immortalized HOSE cells (IHOSE1-15, 12, 636, and 642) [16] and hTERT-immortalized HOSE cells (IOSE20, 21, and 25) [17] were also used in this study.

Three-dimensional Organoid Model of Normal HOSE Cells

The method of our three-dimensional (3D) organoid model of normal HOSE cells was modified from MCF-10A mammary epithelial spheroid model as described by Debnath et al. [18]. Eight-well glass-chambered slides (Nalge Nunc International, Naperville, IL) were coated with growth factor–reduced Matrigel matrix without phenol red (BD Biosciences, Bedford, MA) per well and left to solidify. Primary culture of normal HOSE cells was trypsinized and resuspended in complete medium with 10% FBS and 2% Matrigel. Twenty thousand normal HOSE cells were seeded onto each Matrigel-coated well. Complete medium with 2% Matrigel was replaced every 4 days. For TNF-α treatment, 10 ng/ml of recombinant human TNF-α was added to the culture medium at day 4. TNF-α and fresh media were replaced every 4 days, and the organoid cultures were harvested at day 40.

Immunofluorescent Staining

Control HOSE spheroids and TNF-α–treated cystic structures in Matrigel were fixed in 2% paraformaldehyde. Fixed spheroids were permeabilized with PBS containing 0.5% Triton X-100 and washed three times with 0.1% Triton X-100 in PBS. The washed spheroids were blocked with PBS containing 0.2% BSA and 10% normal goat serum (Jackson ImmunoResearch, West Grove, PA). Primary antibodies were diluted in IF buffer (PBS containing 0.2% BSA and 1% normal goat serum) and incubated. Unbound primary antibodies were removed by PBS washing. Secondary antibodies coupled with Alexa Fluor 647 (Molecular Probes, Eugene, OR) and Alexa Fluor 546 phalloidin (Molecular Probes) were diluted in IF buffer and incubated with the spheroids. Unbound secondary antibodies were washed. The spheroids were then postfixed with 2% paraformaldehyde and counterstained with 1 μg/ml 4′,6-diamidino-2-phenylindole (DAPI) (Molecular Probes). Microscopic images were captured and analyzed by Leica DMIRE2 fluorescence microscope (Leica Microsystems, Bannockburn,

IL) and OpenLab software (Improvision, Lexington, MA). Twenty z-section images (0.5-μm interval) were taken from each spheroid. The images were then deconvoluted by Volocity software (Improvision). For epithelial inclusion cysts in human ovarian cortex, frozen sections (7 μm) of normal ovaries were used for immunofluorescent staining.

Electronic Microscopy

Spheroids of normal HOSE cells were harvested at day 40, fixed in 2.5% glutaraldehyde in 0.1 M phosphate buffer, and processed for transmission electron microscopy (TEM) analysis as described [7].

Diameter Measurement and Cell Proliferation Assay of HOSE Spheroids

The longest diameter of each control HOSE spheroid and TNF-α–treated cystic structures was measured by OpenLab software (Improvision). The data were compared using nonparametric Mann-Whitney *U* test. The level of critical significance was set at $P < .05$. The analyses were performed using SPSS version 10.0 (SPSS, Inc., Chicago, IL). Cell proliferation rates of HOSE cells in organoid cultures (days 7, 14, and 40) were determined by CellTiter 96 nonradioactive cell proliferation assay (Promega, Madison, WI).

Semiquantitative and Real-time Reverse Transcription–Polymerase Chain Reaction

Total RNA of control HOSE spheroids and TNF-α–treated cystic structures was isolated by TriZOL reagent (Invitrogen) and subsequently purified by RNeasy Micro kit (Qiagen, Valencia, CA). The quantity of the isolated RNA was determined by Quant-iT RiboGreen Assay kit (Molecular Probes). Fifteen nanograms of total RNA was then amplified and reverse-transcribed by Ovation Aminoallyl RNA amplification and labeling system (NuGEN Technologies, Inc., San Carlos, CA). A ten-fold dilution of amplified cDNA was used for quantitative polymerase chain reaction (PCR). For semiquantitative reverse transcription (RT)–PCR analysis of *MMP* and tissue inhibitor of metalloproteinase (*TIMP*) genes, human *MMP* gene family I and II MultiGene-12 RT-PCR profiling kits were used (SuperArray, Frederick, MD). For real-time RT-PCR, probes and primer sets for human COL41A, COX-2, CXCR4, DAB2, IL-1β, and MMP-10 were obtained from Taqman Gene Expression Assays (Applied Biosystems, Foster City, CA). Human PPIA (cyclophilin A) was used as endogenous control. Real-time PCR was performed by 7300 real-time PCR systems (Applied Biosystems). All reactions were performed in triplicate. The transcription level of each gene of the treated samples was compared with that of control by $2^{(-\Delta\Delta CT)}$ calculation [19].

Cell Viability Assay

After treatment with TNF-α, the monolayer cell cultures of IOSE25 cells were trypsinized. Viable cells were counted by Vi-Cell XR cell viability analyzer (Beckman Coulter, Miami, FL).

Results

Formation of Spheroids of Normal HOSE Cells in 3D Matrix

To obtain a relevant model for studying the early events of ovarian cancer, we established a unique 3D *in vitro* organoid model of normal HOSE cells. In this model, normal HOSE cells were obtained from the surface of human ovaries from patients with benign gynecological diseases. First passages of monolayer culture of primary normal HOSE cells were harvested for the *in vitro* organoid model (Figure 1*A*). To ensure the quality of epithelial cells in primary cultures, the cell cultures were immunofluorescent stained with ovarian epithelial markers (cytokeratins AE1&3 and calretinin). Normal HOSE cells in primary cultures presented a compact and cobblestone-like pattern and were positive for cytokeratins and calretinin (Figure 1*B*). The primary cultures with more than 95% of normal HOSE cells were used for subsequent 3D culture.

For 3D organoid model, single-cell suspension of normal HOSE cells was seeded onto the matrix. Cell aggregates were formed within the matrix after 2 days. After the 40-day culture, spheroids of normal HOSE cells with single epithelial lining and hollow lumen were formed (Figure 1*C*). Using our method, in general, 70% of HOSE samples from different patients were able to grow spheroids. Approximately 20 spheroids of normal HOSE cells were formed in each well of eight-well glass-chambered slides. The sizes of the spheroids varied, which were dependent on the number of normal HOSE cells aggregated. Most of the normal HOSE cells ended up as constituents of the spheroids, whereas only a very small amount of cells remained single in the matrix. In addition, all of the spheroids were found to be developed with a lumen.

The morphogenesis of spheroids of the normal HOSE cells was investigated by immunofluorescent staining of a cell proliferation marker (Ki-67) and an apoptotic marker (active caspase-3). Ki-67–positive cells were not detected in the spheroids throughout 40-day culture. This result indicated that normal HOSE cells of the spheroids are in a growth-arrested status. On the contrary, activated caspase 3–positive cells were detected in the internal luminal cells but not in the outer cell layer of the spheroids. This result suggested that apoptosis contributes to the lumen formation of the spheroids of normal HOSE cells (Figure 1*D*).

Besides Ki-67 and activated caspase 3, the morphogenesis of normal HOSE spheroids was further analyzed by several specific antibodies, which have been used to characterize the 3D *in vitro* MCF-10A mammary acini [18]. E-cadherin (ECAD), a protein for cell-cell junctions, was expressed in the normal HOSE cells of the spheroids at days 2 and 7. However, the expression of ECAD was lost in the epithelium of spheroids at days 14 and 40. Collagen type IV (COL4), a component of basement membrane, was absent in normal HOSE spheroid at day 2, but COL4 was expressed at basal surface of normal HOSE spheroids at days 7, 14, and 40. This result indicated that the development of basement membrane, which surrounds the spheroid of normal HOSE cells, is started beyond day 2 of the culture. The ERM proteins play a role in regulate cell size/shape and are located in actin-rich structures. At day 2 of the culture, ERM proteins were evenly expressed in the spheroid of normal HOSE cells. However, the expression of ERM proteins was distinctively localized at the basal surface of HOSE spheroids at the culture days 7, 14, and 40 (Figure 2*A*). The expression pattern of ERM proteins was similar to that of F-actin during the development of HOSE spheroids (Figure 1*C*). On the basis of the localizations of ERM proteins and F-actin, our results suggested that epithelial polarity is established in normal HOSE spheroid during the morphogenesis.

In Vitro *Spheroids of Normal HOSE Cells Resembles* In Vivo *Epithelial Inclusion Cyst in Human Ovarian Cortex*

The characteristic of mature spheroids of the normal HOSE cells (day 40) was further examined by TEM and other immunofluorescent

staining. In semithin section of the spheroid, a single epithelial lining of flat cells was observed. By TEM, a basement membrane was detected at the basal surface of the ovarian epithelium (Figure 2*B*). The basement membranes in the mature spheroids were also shown by basal expression of COL4 and HSPG. The epithelial lining of the spheroids was polarized as indicated by apical localization of a Golgi marker GM130. In addition, epithelium of the mature spheroids maintained expression of calretinin (Figure 2*C*).

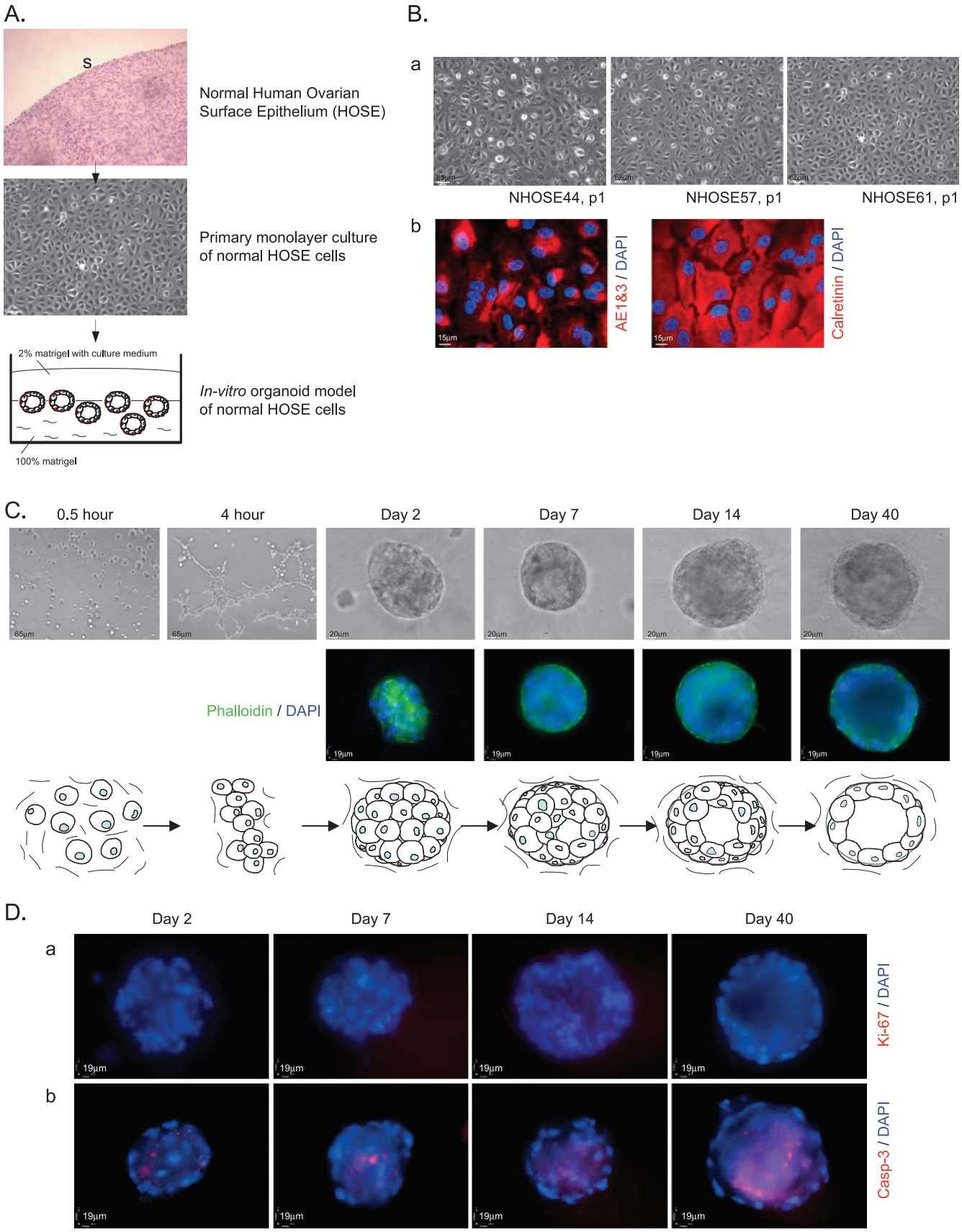

Parallel immunofluorescent experiments were performed on the frozen sections of an *in vivo* epithelial inclusion cyst in the human ovarian cortex. The results showed that human ovarian inclusion cyst was consisted of a single epithelium of flat cells, which expressed cytokeratins (AE1&3) and calretinin (Figure 2*C*). GM130 was located at the apical surface of the epithelium, whereas the components of basement membrane (laminin V, HSPG, and COL4) were expressed at the basal surface of the epithelium of ovarian inclusion cyst (Figure 2*C* and data not shown). Because the protein expression, localization, and morphology of *in vivo* human ovarian inclusion cyst are similar to those of *in vitro* normal HOSE spheroids, the results suggested that the normal HOSE spheroid model system resembles *in vivo* human ovarian inclusion cysts.

Immortalized HOSE Cell Lines Fail to Form Simple Spheroids in Matrix

The HPV E6/E7– or hTERT-immortalized HOSE cell lines are useful nonmalignant tools for the studies of ovarian carcinogenesis [16,17]. Therefore, we attempted to use these immortalized nonmalignant HOSE cells for the *in vitro* organoid model. Our results showed that HPV E6/E7–immortalized cell lines (IHOSE1-15, IHOSE12, and IHOSE636) failed to form simple spherical structures in the matrix. They formed disorganized aggregates with irregular epithelial polarity and mild protrusion instead (Figure 3*A*). For hTERT-immortalized HOSE cell lines, three of them (IOSE20C2, IOSE21C21, and IOSE25C2) formed disorganized structures in the matrix, whereas the IOSE25C26 cells remained a scattering of small cell masses in the matrix (Figure 3*B*).

TNF-α Induces Enlargement of the Spheroids of HOSE Cells by Reinitiating Proliferation

To investigate the role of inflammatory cytokine TNF-α on malignant transformation of the normal ovarian epithelium, the spheroids of normal HOSE cells were treated with a protumor dose of TNF-α (10 ng/ml) for 36 days. After TNF-α treatment, sizes of the treated cystic structures were significantly larger than that of the control HOSE spheroids (Figure 4, *A* and *B*). MTT assay demonstrated that the cell proliferation rates of TNF-α–treated cystic structures were significantly higher than that of the control at culture days 15 and 40, respectively (Figure 4*C*). Positive Ki-67 cells were also detected in TNF-α–treated cystic structures at day 15 (Figure 4*D*). These results indicated that TNF-α causes enlargement of the spheroids by reinitiating proliferation. This TNF-α–induced cell proliferation was also correlated with the up-regulation of a protumor cytokine, IL-1β, in the TNF-α–treated cystic structures (Figure 4*E*).

TNF-α Induces Disorganization, Multilayer Stratification, Disruption of Epithelial Polarity, and Disintegration of Basement Membrane in Ovarian Epithelial Cystic Structures

By immunofluorescent staining of ERM proteins, disorganization and multilayer stratification in the TNF-α–treated cystic structures were observed. Moreover, the expression of ERM proteins in the TNF-α–treated cystic structures was not restricted at the basal surface but spread throughout the structures (Figure 4*F*). Expression of GM130 was also no longer restricted at the apical surface of the TNF-α–treated cystic structures (Figure 5*B*). These results suggested that TNF-α induces disruption of epithelial polarity in the cystic structures. In addition, the expressions of COL4 (Figure 5*A*) and HSPG (Figure 5*B*) at the basal surface of the cystic structures were significantly lost after TNF-α treatment. These results suggested that TNF-α induces disintegration of basement membrane in ovarian epithelial cystic structures. The loss of basement membrane in the TNF-α–treated cystic structures was correlated with the down-regulation of transcript level of COL4 (*COL4A1*; Figure 5*B*).

Because basement membranes are degraded by MMPs in tumor progression, we compared the expression levels of *MMP* and *TIMP* genes in control HOSE spheroids and TNF-α–treated cystic structures. Our result demonstrated that messenger RNA (mRNA) and protein expressions of MMP-10 (stromelysin 2) were significantly higher in the TNF-α–treated cystic structures when compared with the normal control (Figure 5, *C* and *D*). This result suggested that the basement membrane of HOSE spheroid may be disintegrated by MMP-10 during TNF-α treatment.

TNF-α Induces Invasive Phenotype in Ovarian Epithelial Cystic Structures

After TNF-α treatment, expression of F-actin was no longer confined at the basal surface of the cystic structure. Actin rearrangement and cellular protrusion were found in TNF-α–treated cystic structures instead (Figure 6*A*). These observations indicated that TNF-α induces invasive phenotype in the cystic structures. Because chemokine receptor CXCR4 is critical to tumor cell migration and is regulated by TNF-α in ovarian cancer cells [20], we examined the mRNA expression of CXCR4 in the cystic structures after TNF-α treatment. Up-regulation of CXCR4 transcript was found in TNF-α–treated cystic structures when compared with the control HOSE spheroids (Figure 6*B*). These results suggested that TNF-α upregulates CXCR4 in the ovarian epithelial cells and promoted cell migration from the ovarian cystic structures to extracellular matrix.

Although the E6/E7–immortalized HOSE cells did not form simple spherical structures in the control experiments (Figure 3*A*), TNF-α also induced larger, prominently disorganized and extensive invasive phenotypes in the *in vitro* organoid model of E6/E7–immortalized HOSE

Figure 1. *In vitro* organoid model of normal HOSE cells. (A) Schematic diagram to show the experimental procedure of the *in vitro* organoid model of normal HOSE cells. Normal HOSE cells were obtained by cytobrushing the surface epithelium (S) of normal ovary and were subsequently cultured. First passages of the primary cultures of normal HOSE cells were harvested for 3D *in vitro* cultures. (B) Phase-contrast images of three representative monolayer cultures of primary normal HOSE cells (a); Immunofluorescent staining of cytokeratin (AE1&3) and calretinin in monolayer cultures of primary normal HOSE cells (b). (C) Morphogenesis of spheroids of normal HOSE cells in 3D matrix. Upper panel: phase-contrast images of aggregates and spheroids of normal HOSE cells at different stages of *in vitro* organoid model. Middle panel: fluorescence staining of F-actin and nuclei in aggregates and spheroids of normal HOSE cells at different stages of the culture; F-actin proteins were stained by phalloidin, whereas nuclei were stained by DAPI. Lower panel: schematic diagram of the morphogenesis of the spheroids of normal HOSE cells. (D) Immunofluorescent staining of Ki-67 (a) and activated caspase 3 (b; Casp-3) at different stages of the morphogenesis of spheroids of normal HOSE cells; nuclei were counterstained by DAPI.

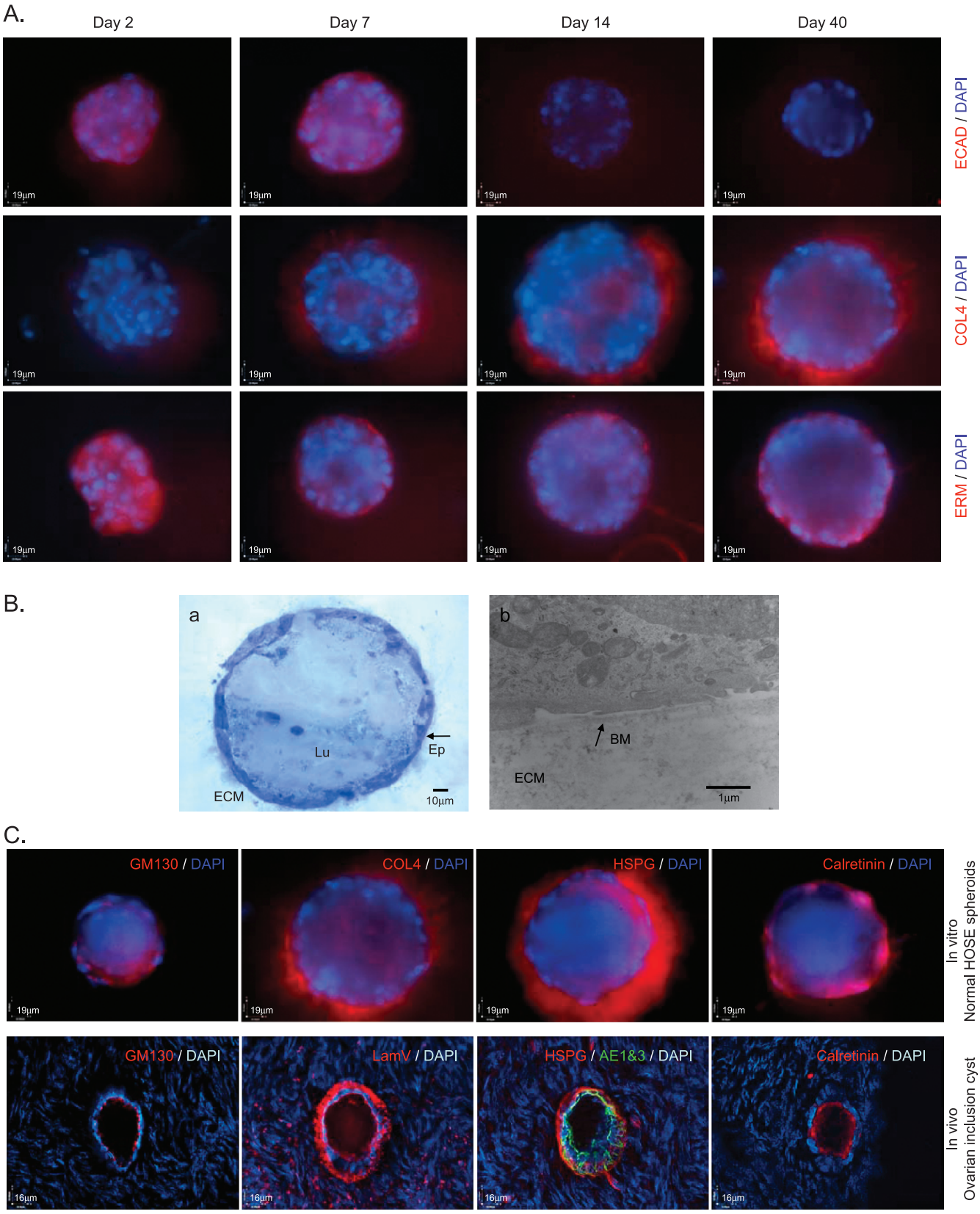

Figure 2. Characterization of the spheroids of normal HOSE cells in the matrix. (A) Immunofluorescent staining of ECAD (upper row), COL4 (middle row), and ERM (lower row) at different stages of the morphogenesis of spheroids of normal HOSE cells; nuclei were counterstained by DAPI. (B) Semithin section of the spheroid of normal HOSE cells in the Matrigel (a). *ECM* indicates extracellular matrix; *Ep*, epithelial lining; *Lu*, lumen of spheroid. Transmission electron microscopic imaging of the spheroid of normal HOSE cells (b). *BM* indicates basement membrane (arrow); *ECM*, extracellular matrix. (C) Upper panel: immunofluorescent staining of GM130, COL4, HSPG, and calretinin of *in vitro* normal HOSE spheroids. Lower panel: immunofluorescent staining of GM130, laminin V (LamV), HSPG, cytokeratin (AE1&3), and calretinin of an *in vivo* ovarian inclusion cyst.

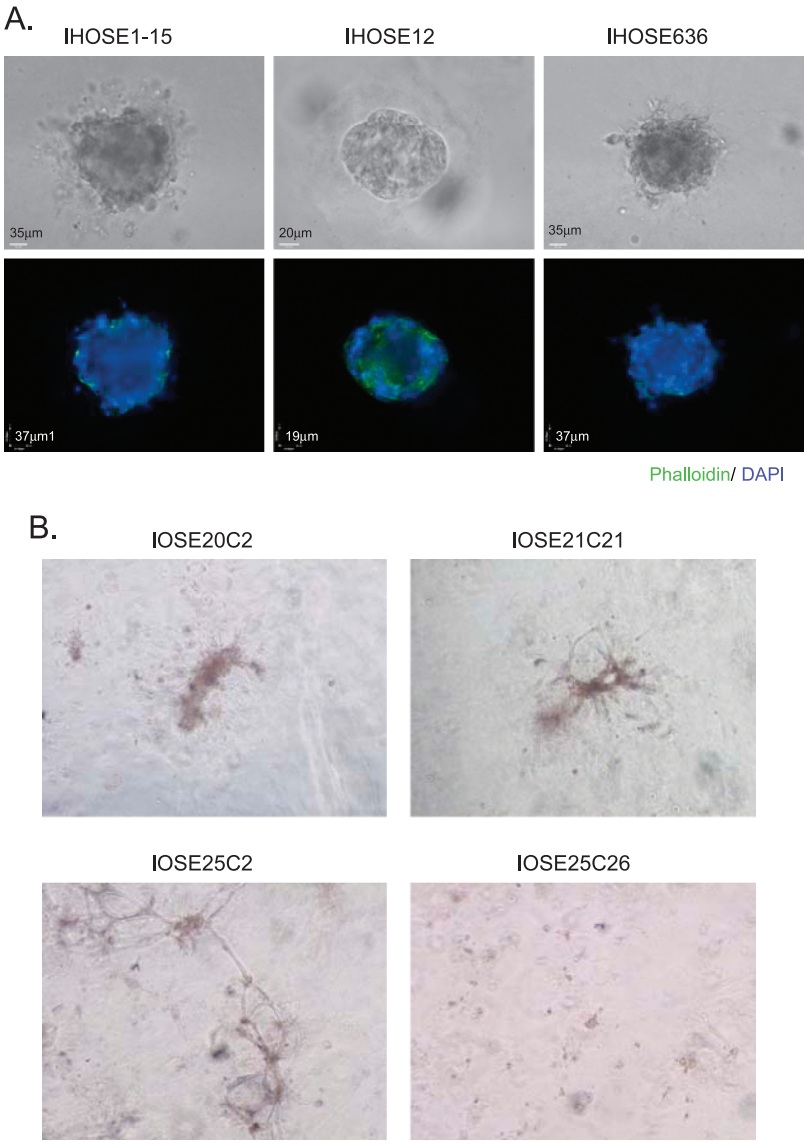

Figure 3. Three-dimensional *in vitro* culture of immortalized HOSE cells. (A) Three-dimensional *in vitro* organoid model of HPV E6/E7–immortalized HOSE cells. Upper panel: phase-contrast images of the cystic structures of E6/E7–immortalized HOSE cells in the matrix. Lower panel: fluorescence staining of F-actin and nuclei in the cystic structures of E6/E7–immortalized HOSE cells. (B) Phase-contrast images of 3D *in vitro* cultures of hTERT-immortalized HOSE cells in the matrix.

cells (Figure 6*C*). Taken together, these results indicated that TNF-α induces cell migration and invasion of ovarian epithelial cells of the cystic structures.

TNF-α Upregulates Ovarian Cancer Markers in Ovarian Epithelial Cystic Structures

The overexpression of ovarian cancer markers (CA125, MUC1, EpCAM, and claudin 4) was detected in the TNF-α–treated ovarian cystic structures when compared with the control HOSE spheroids (Figure 6*D*).

Collectively, our results demonstrated that the TNF-α–treated cystic structures exhibit characteristics of precancerous ovarian lesions.

TNF-α Fails to Induce Cell Proliferation in Monolayer Culture of Immortalized HOSE Cells

To study the effect of TNF-α on monolayer cell culture of HOSE cells, we treated the monolayer cell culture of IOSE25 cells with TNF-α (10 ng/ml) for 5 days. Cell viability and CXCR4 expression were examined after the treatment. Up-regulation of CXCR4 was detected in monolayer cell culture of IOSE25 cells after treatment with TNF-α; however, no TNF-α–induced cell proliferation could be found in monolayer cell cultures of IOSE25 cells (Figure 6*E*). The discrepancy between the monolayer cell culture and the spheroid culture model suggested that the latter is a better model as a precursor of ovarian cancer.

Discussion

In the present study, we established an organoid model of normal HOSE cells, which recapitulates the epithelial inclusion cyst in human ovarian cortex. The resemblance of this *in vitro* organoid model to an epithelial inclusion cyst constitutes a useful tool for investigating the roles of oncogenes, tumor suppressors, and extrinsic factors for ovarian tumor development.

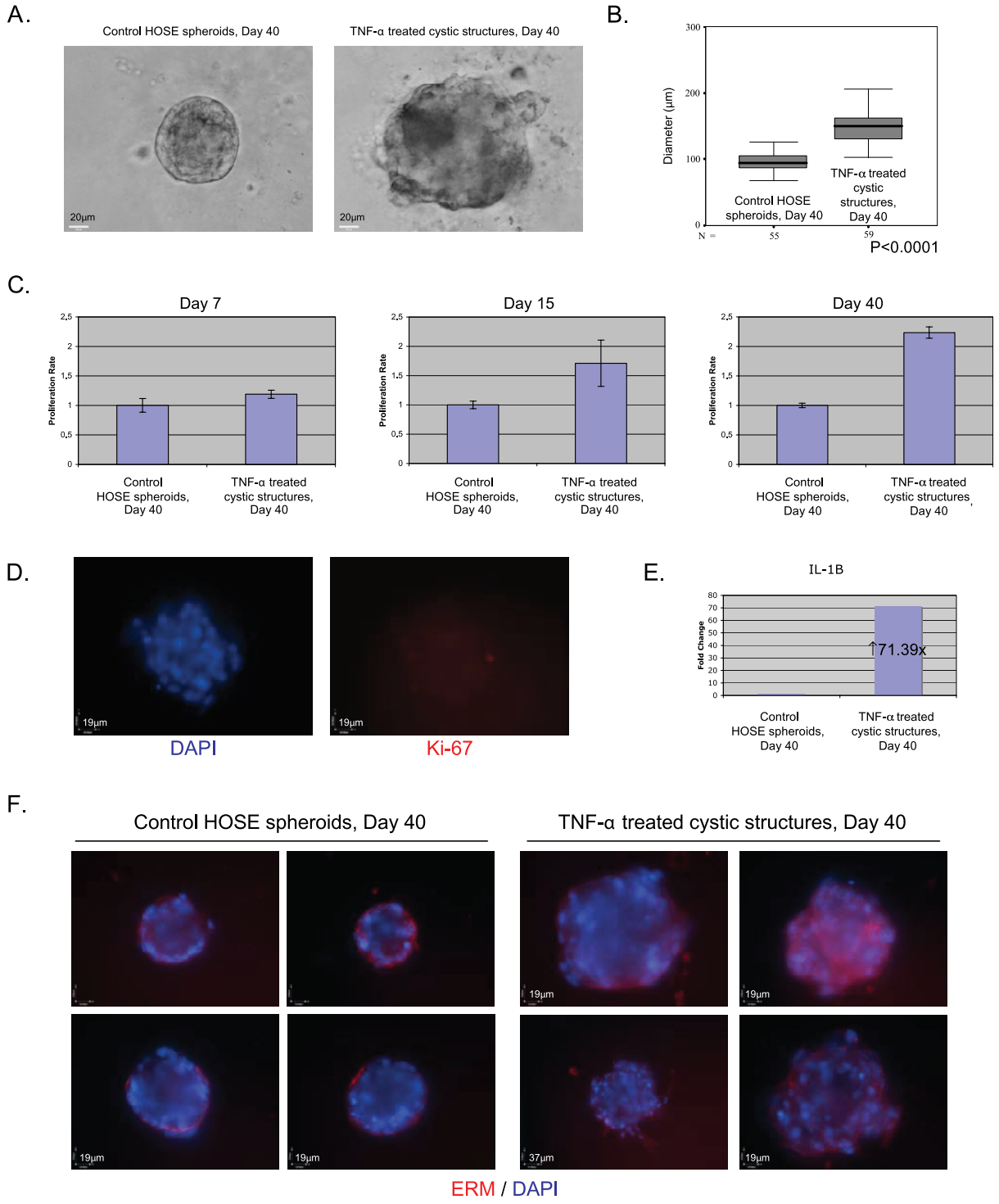

Figure 4. Tumor necrosis factor α induced enlargement, disorganization, multilayer stratification, and disruption of cell polarity in ovarian epithelial cystic structures. (A) Representative phase-contrast images of normal HOSE spheroids and TNF-α–treated cystic structures at culture day 40. Scale bar, 20 μm. (B) Statistical analysis of diameters (in μm) of control HOSE spheroids (n = 55) and TNF-α–treated cystic structures (n = 59) at day 40. The box is bounded above and below by the 75th and 25th percentiles; the median is indicated by the line in the box. Statistical analysis was performed using nonparametric Mann-Whitney U test. (C) MTT assay of control HOSE spheroids and TNF-α–treated cystic structures at culture days 7, 15, and 40. The cell proliferation rate of the TNF-α–treated group was normalized to that of the control group. Bars, SE. (D) Immunofluorescent staining of Ki-67 in TNF-α–treated cystic structures at day 15: DAPI stain (left) and Ki67 immunostaining (right). (E) Quantitative RT-PCR analysis of *IL-1β* gene in control HOSE spheroids and TNF-α–treated cystic structures at day 40. The transcript level of the target genes in TNF-α–treated cystic structures was normalized to that in the control HOSE spheroids using $2^{(-\Delta\Delta CT)}$ calculation. (F) Immunofluorescent staining of ERM in control HOSE spheroids and TNF-α–treated cystic structures at day 40; four representative images of each treatment are shown.

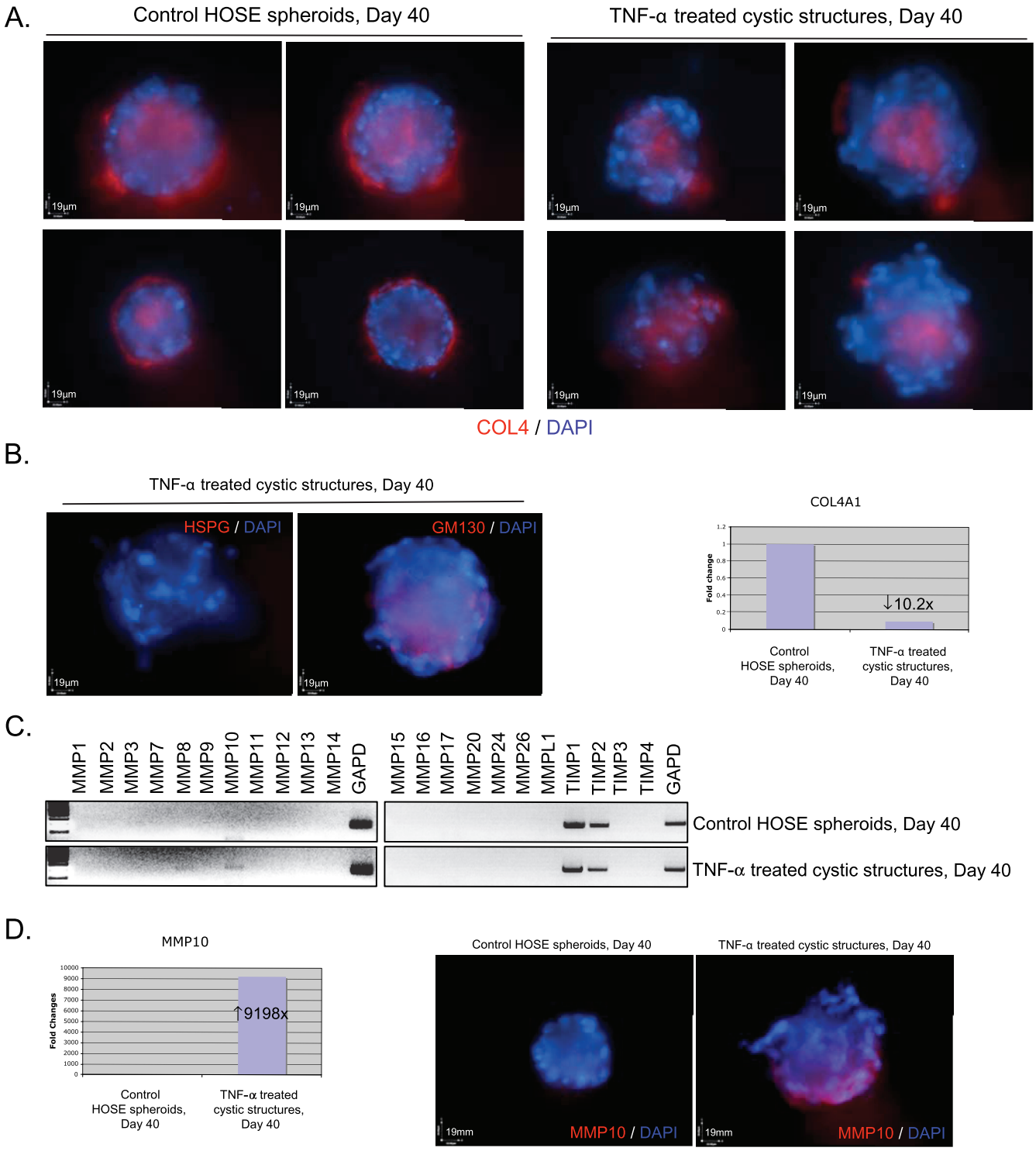

Figure 5. Tumor necrosis factor α induced disintegration of basement membrane and expression of MMP-10 in ovarian epithelial cystic structures. (A) Immunofluorescent staining of COL4 in control HOSE spheroids and TNF-α–treated cystic structures at day 40; four representative images of each treatment are shown. (B) Left panel: immunofluorescent staining of HSPG and GM130 in TNF-α–treated cystic structures at day 40. Right panel: quantitative RT-PCR analysis of COL4 (*COL4A1*) gene in control HOSE spheroids and TNF-α–treated cystic structures at day 40. The transcript level of the target genes in TNF-α–treated cystic structure was normalized to that in the control HOSE spheroids using $2^{(-\Delta\Delta CT)}$ calculation. (C) Semiquantitative RT-PCR analysis of *MMP* and *TIMP* genes in control HOSE spheroids and TNF-α–treated cystic structures at day 40. Expression of GAPD was served as control of mRNA input. (D) Up-regulation of MMP-10 in TNF-α treatment of the HOSE spheroids. Left panel: quantitative RT-PCR analysis of *MMP-10* gene in control HOSE spheroids and TNF-α–treated cystic structures at day 40. Right panel: representative results of immunofluorescent staining of MMP-10 protein in control HOSE spheroids and TNF-α–treated cystic structures at day 40.

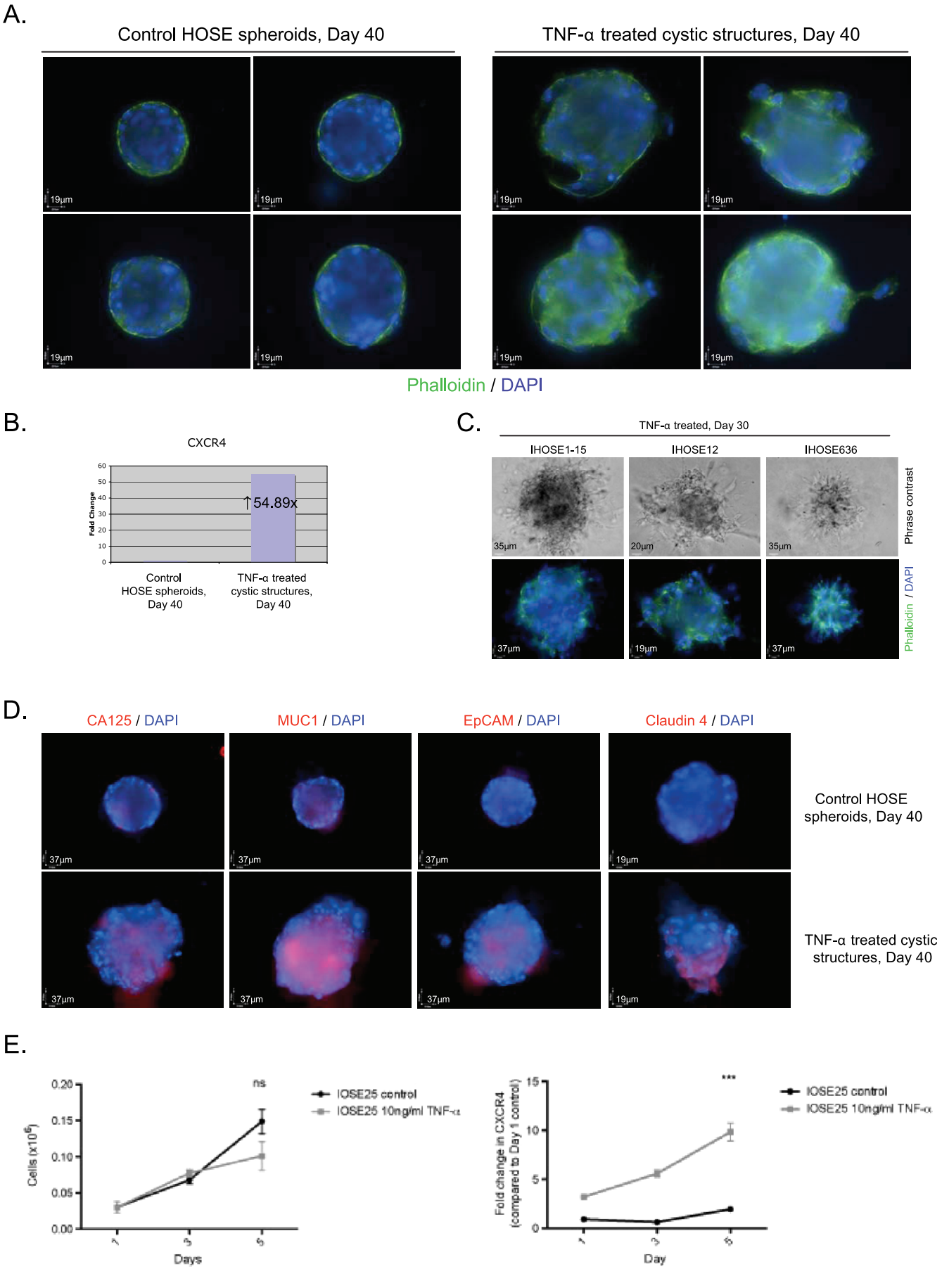
A.
Control HOSE spheroids, Day 40
TNF-α treated cystic structures, Day 40
19μm
Phalloidin / DAPI
B.
CXCR4
Fold Change
60
50
40
30
20
10
0
↑54.89x
Control HOSE spheroids, Day 40
TNF-α treated cystic structures, Day 40
C.
TNF-α treated, Day 30
IHOSE1-15
IHOSE12
IHOSE636
35μm
20μm
37μm
19μm
Phrase contrast
Phalloidin / DAPI
D.
CA125 / DAPI
MUC1 / DAPI
EpCAM / DAPI
Claudin 4 / DAPI
Control HOSE spheroids, Day 40
TNF-α treated cystic structures, Day 40
E.
Cells (x10^6)
0.20
0.15
0.10
0.05
0.00
ns
IOSE25 control
IOSE25 10ng/ml TNF-α
Days
Fold change in CXCR4 (compared to Day 1 control)
15
10
5
0
***
IOSE25 control
IOSE25 10ng/ml TNF-α
Day

The formation of epithelial inclusion cysts *in vivo* is not fully understood. The proposed origins of the epithelial inclusion cysts are the fragments of OSE, which are trapped in or near ruptured follicles at the time of ovulation [21,22], or invaginations of the OSE into the stroma of the ovary as a result of ovulation and aging [5]. The histologic diagnosis of OSE cells lining the regularly shaped inclusion cysts *in vivo* was flat to cuboidal [23], which is similar to that of the spheroids of normal HOSE cells in our organoid model. On the contrary, the population of OSE cells in irregularly shaped inclusion cysts *in vivo* was heterogeneous, i.e., a combination of normal flat-to-cuboidal OSE cells, columnar OSE cells, and intermediate stages between cuboidal and columnar types of OSE cells was observed [23]. Such irregularly shaped inclusion cysts were often found in ovarian tissues obtained from patients undergoing oophorectomy for genital tract pathology and from patients with a family history of breast and/or ovarian cancer [23]. These observations highly suggested that the irregularly shaped inclusion cysts *in vivo* are the precancerous (dysplastic) lesions of ovarian epithelial malignancy [24].

Ovarian epithelial dysplasia was first described after prophylactic oophorectomies for genetic risk. Ovarian dysplasia in epithelial inclusion cysts of the high-risk population has also been described [24–26]. In a previous study, the normal identical twin sisters of the patients with ovarian cancer were subjected to prophylactic oophorectomy after menopause. Histological examination of these ovarian tissues revealed dysplastic changes in epithelial inclusion cysts, including transition of epithelial inclusion cysts from cuboidal to tall columnar ciliated epithelium, cellular stratification, loss of polarity, and epithelial tufting [26]. The finding of epithelial abnormality suggested a precancerous change in epithelial inclusion cysts similar to other genital epithelial dysplasia [24,26]. Several other cancerous features, such as loss of basement membrane, loss of Dab-2 expression, overexpression of Cox-2, Ki-67, and tumor markers, were also detected in epithelial inclusion cysts of the high-risk patients [23,27,28]. Taken together, these results suggested that the precancerous lesion might arise at the epithelial inclusion cysts, which have been exposed to the stimuli of ovarian stromal microenvironment [29]. Although two recent reviews have suggested that fallopian tube fimbria is a field of origin for high-grade serous carcinoma of the ovary as well as ovarian epithelial tumors that arose from tissues that are embryonically derived from the müllerian ducts (i.e., fallopian tubes, endometrium, and endocervix) [30,31], we cannot rule out the fact that OSE cells are one of the cell origins of ovarian epithelial cancer.

More interestingly, the TNF-α–treated ovarian cystic structures in our experiment shared the similarities (i.e., epithelial stratification, loss of epithelial polarity, loss of basement membrane, loss of Dab-2 expression, overexpression of Ki-67, overexpression of Cox-2, and overexpression of tumor markers) that are found in the ovarian dysplasia of epithelial inclusion cysts of the high-risk patients. These similarities suggest that the TNF-α–treated ovarian cystic structures exhibit characteristics of precancerous lesions of ovarian epithelial malignancy.

Tumor necrosis factor α (TNF-α) was originally identified and characterized by its ability to induce necrosis in tumor with high-dose administration [32,33]. Follow-up studies demonstrated that sustained production of TNF-α in the tumor microenvironment could promote progression of tumor cells [34–37]. It has also been shown that TNF-α is a potent tumor promoter in BALB/3T3 cell transformation during cotreating the cells with the chemical carcinogen 3-methylcholanthrene and TNF-α [38]. Other studies using mice deficient in TNF-α showed that TNF-α could promote the progression of skin carcinogenesis induced by carcinogen [39–41], whereas its molecular actions in such tumor progression included 1) induction of DNA damage and subsequent gene mutations by increasing reactive oxygen species [42,43], 2) stimulation of epithelial-to-mesenchymal transition by activating p38 MAPK and ERK activity [44], 3) induction of invasiveness and adhesion of the epithelial cells by enhancing the expression of MMP-9 and α_2 integrin [45], and 4) enhancement of metastasis of tumor cells [46–49].

Tumor necrosis factor α plays a role in ovarian cancer has been known for more than two decades. Tumor necrosis factor α and its receptors are expressed in human ovarian cancers [50]. Studies showed that TNF-α induced autocrine production of TNF-α and cell growth in OSE cells [14,51,52]. However, when we treated the monolayer cell culture of immortalized HOSE cells with TNF-α, no TNF-α–induced cell proliferation was found in the monolayer cultures of immortalized HOSE cells. The discrepancy between these studies may be due to the difference in doses of TNF-α for *in vitro* treatments. Yang et al. [13] reported that treatment of TNF-α in immortalized HOSE cells would degrade the components of basement membrane (COL4 and laminin) through increasing the activity of urokinase-type plasminogen activator and MMP-9. However, no study has yet been reported that TNF-α could confer malignant transformation in normal HOSE cells. In ovarian cancer cells, TNF-α upregulated the expression of chemokine receptor CXCR4 through activating the components of the NF-κB pathway [20]. Furthermore, knockdown of TNF-α in ovarian cancer cells reduced the production of tumor-promoting cytokines and chemokines, tumor growth and metastasis, growth of endothelial cells, and vascularization of the tumor [15]. Taken together, TNF-α may enhance tumor growth and invasion by inducing the secretion of cytokines, proangiogenic factors, and metalloproteinases.

The results of these basic medical research encouraged phase 1 clinical studies on the treatment of ovarian cancer with TNF-α inhibitors. Thalidomide is a drug that inhibits the processing of the mRNA of a number of peptide-signaling molecules such as TNF-α. The use of thalidomide was investigated in 19 patients with ovarian cancer. One of the patients experienced stabilization of disease for more than 3 months [53]. Etanercept is a recombinant human soluble p75 TNF

Figure 6. Tumor necrosis factor α induced invasive phenotypes and overexpression of ovarian cancer markers in ovarian epithelial cystic structures. (A) Fluorescence labeling of F-actin (phalloidin) and nuclei (DAPI) in control HOSE spheroids and TNF-α–treated cystic structures at day 40; four representative images of each treatment are shown. (B) Quantitative RT-PCR analysis of CXCR4 in control HOSE spheroids and TNF-α–treated cystic structures at day 40. (C) Tumor necrosis factor α treatment on the cystic structures of HPV E6/E7–immortalized HOSE cells in the matrix for 30 days. Upper panel: phase-contrast images of the cystic structures of E6/E7–immortalized HOSE cells after TNF-α treatment. Lower panel: fluorescence staining of F-actin (phalloidin) and nuclei (DAPI) of the cystic structures after TNF-α treatment. (D) Immunofluorescent staining of ovarian cancer markers (CA125, MUC1, EpCAM, and claudin 4) in control HOSE spheroids and TNF-α–treated cystic structures at day 40. (E) Left panel: cell viability assay in IOSE25 cells in the presence of TNF-α (0 and 10 ng/ml) for 1, 3, and 5 days. Right panel: quantitative RT-PCR of CXCR4 in IOSE25 cells in the presence of TNF-α (0 and 10 ng/ml) for 1, 3, and 5 days. Bars, SE. *ns* indicates not significant. ***Statistically significant as analyzed by repeated ANOVA.

receptor that binds to TNF-α. Treatment with etanercept has been investigated in 30 patients with recurrent ovarian cancer. Eighteen of the 30 patients completed the treatment. Six patients achieved prolonged disease stabilization, and a significant rise in immunoreactive TNF-α was seen in all patients [54]. These results indicated that the effect of the TNF-α inhibitors is limited in ovarian cancer treatment. The reason may be that the inhibition of TNF-α is compensated by other members in cytokine network of ovarian tumor microenvironment [15].

This report has mainly investigated the role of TNF-α in tumor initiation from the organoid model of normal HOSE cells. Our results demonstrated that TNF-α conferred precancerous phenotype in the normal HOSE spheroids. These data further supported the link between chronic inflammation and ovarian carcinogenesis, particularly in tumor initiation, and illustrated that this precancerous phenotype is arisen from the site mimicking the epithelial inclusion cysts. However, our results also reflected that TNF-α alone could not completely transform the normal HOSE cells to malignant phenotypes. In this case, we suggest that other protumor cytokines, such as IL-1β and IL-6, are needed for the malignant transformation of normal HOSE cells. It is also possible that cellular senescence would occur in the TNF-α–treated ovarian cystic structures if there are any DNA damage and oncogenic signals in HOSE cells, which are induced by the cytokine. Because cells enter senescence in response to a variety of cellular stress, including telomere erosion, DNA damage, and oncogenic signals, cellular senescence could act as a barrier against malignant transformation. If this happens, it will be another reason why TNF-α alone could not induce malignant transformation of normal HOSE cells. Indeed, cellular senescence is frequently present in precancerous lesion of tumors [55]. Therefore, a future study is needed to investigate whether TNF-α could induce cellular senescence in the HOSE spheroids.

Besides, it is commonly known that tumor mass is not solely composed of tumor cells; the microenvironment of tumor consists of different cell types. Because tumor microenvironment would influence tumor progression and metastasis, lack of stromal components (e.g., fibroblasts) in the 3D organoid model may be a factor that contributes to the failed transformation of normal HOSE cells.

In summary, we believe that our organoid model of normal HOSE cells is a relevant model for ovarian cancer research because the epithelial inclusion cysts are thought to be the site of origin of the disease [6,56]. More importantly, this model may be very useful in studying the pathogenesis of ovarian cancer, and the results indicate that inflammation may be important in ovarian carcinogenesis.

References

[1] Rosenthal A and Jacobs I (1998). Ovarian cancer screening. *Semin Oncol* **25**, 315–325.

[2] Bell D and Scully R (1991). *Clinical Perspective on Borderline Tumors of the Ovary.* New York, NY: Elsevier Science Publishing Co. Inc, pp. 119–133.

[3] Seidman J, Russell P, and Kurman R (2002). *Surface Epithelial Tumors of the Ovary.* New York, NY: Springer, pp. 791–904.

[4] Blaustein A (1981). Surface cells and inclusion cysts in fetal ovaries. *Gynecol Oncol* **12**, 222–233.

[5] Scully RE (1995). Pathology of ovarian cancer precursors. *J Cell Biochem* **23**, 208–218.

[6] Auersperg N, Wong AS, Choi KC, Kang SK, and Leung PC (2001). Ovarian surface epithelium: biology, endocrinology, and pathology. *Endocr Rev* **22**, 255–288.

[7] Kwong J, Choi HL, Huang Y, and Chan FL (1999). Ultrastructural and biochemical observations on the early changes in apoptotic epithelial cells of the rat prostate induced by castration. *Cell Tissue Res* **298**, 123–136.

[8] Giudice LC and Kao LC (2004). Endometriosis. *Lancet* **364**, 1789–1799.

[9] Merritt MA, Green AC, Nagle CM, and Webb PM (2008). Talcum powder, chronic pelvic inflammation and NSAIDs in relation to risk of epithelial ovarian cancer. *Int J Cancer* **122**, 170–176.

[10] Ness RB, Grisso JA, Cottreau C, Klapper J, Vergona R, Wheeler JE, Morgan M, and Schlesselman JJ (2000). Factors related to inflammation of the ovarian epithelium and risk of ovarian cancer. *Epidemiology* **11**, 111–117.

[11] Schildkraut JM, Moorman PG, Halabi S, Calingaert B, Marks JR, and Berchuck A (2006). Analgesic drug use and risk of ovarian cancer. *Epidemiology* **17**, 104–107.

[12] Lin WW and Karin M (2007). A cytokine-mediated link between innate immunity, inflammation, and cancer. *J Clin Invest* **117**, 1175–1183.

[13] Yang WL, Godwin AK, and Xu XX (2004). Tumor necrosis factor-alpha–induced matrix proteolytic enzyme production and basement membrane remodeling by human ovarian surface epithelial cells: molecular basis linking ovulation and cancer risk. *Cancer Res* **64**, 1534–1540.

[14] Wu S, Boyer CM, Whitaker RS, Berchuck A, Wiener JR, Weinberg JB, and Bast RC Jr (1993). Tumor necrosis factor alpha as an autocrine and paracrine growth factor for ovarian cancer: monokine induction of tumor cell proliferation and tumor necrosis factor alpha expression. *Cancer Res* **53**, 1939–1944.

[15] Kulbe H, Thompson R, Wilson JL, Robinson S, Hagemann T, Fatah R, Gould D, Ayhan A, and Balkwill F (2007). The inflammatory cytokine tumor necrosis factor-alpha generates an autocrine tumor-promoting network in epithelial ovarian cancer cells. *Cancer Res* **67**, 585–592.

[16] Tsao SW, Mok SC, Fey EG, Fletcher JA, Wan TS, Chew EC, Muto MG, Knapp RC, and Berkowitz RS (1995). Characterization of human ovarian surface epithelial cells immortalized by human papilloma viral oncogenes (HPV-E6E7 ORFs). *Exp Cell Res* **218**, 499–507.

[17] Li NF, Broad S, Lu YJ, Yang JS, Watson R, Hagemann T, Wilbanks G, Jacobs I, Balkwill F, Dafou D, et al. (2007). Human ovarian surface epithelial cells immortalized with hTERT maintain functional pRb and p53 expression. *Cell Prolif* **40**, 780–794.

[18] Debnath J, Muthuswamy SK, and Brugge JS (2003). Morphogenesis and oncogenesis of MCF-10A mammary epithelial acini grown in three-dimensional basement membrane cultures. *Methods* **30**, 256–268.

[19] Livak KJ and Schmittgen TD (2001). Analysis of relative gene expression data using real-time quantitative PCR and the 2(–Delta Delta C(T)) method. *Methods* **25**, 402–408.

[20] Kulbe H, Hagemann T, Szlosarek PW, Balkwill FR, and Wilson JL (2005). The inflammatory cytokine tumor necrosis factor-alpha regulates chemokine receptor expression on ovarian cancer cells. *Cancer Res* **65**, 10355–10362.

[21] Radisavljevic SV (1977). The pathogenesis of ovarian inclusion cysts and cystomas. *Obstet Gynecol* **49**, 424–429.

[22] Murdoch WJ (1994). Ovarian surface epithelium during ovulatory and anovulatory ovine estrous cycles. *Anat Rec* **240**, 322–326.

[23] Slot KA, de Boer-Brouwer M, Voorendt M, Sie-Go DM, Ghahremani M, Dorrington JH, and Teerds KJ (2006). Irregularly shaped inclusion cysts display increased expression of Ki67, Fas, Fas ligand, and procaspase-3 but relatively little active caspase-3. *Int J Gynecol Cancer* **16**, 231–239.

[24] Deligdisch L, Einstein AJ, Guera D, and Gil J (1995). Ovarian dysplasia in epithelial inclusion cysts. A morphometric approach using neural networks. *Cancer* **76**, 1027–1034.

[25] Feeley KM and Wells M (2001). Precursor lesions of ovarian epithelial malignancy. *Histopathology* **38**, 87–95.

[26] Gusberg SB (1983). The diagnosis of gynecologic cancer. *Cancer* **51**, 2477–2479.

[27] Roland IH, Yang WL, Yang DH, Daly MB, Ozols RF, Hamilton TC, Lynch HT, Godwin AK, and Xu XX (2003). Loss of surface and cyst epithelial basement membranes and preneoplastic morphologic changes in prophylactic oophorectomies. *Cancer* **98**, 2607–2623.

[28] Blaustein A, Kaganowicz A, and Wells J (1982). Tumor markers in inclusion cysts of the ovary. *Cancer* **49**, 722–726.

[29] Cramer DW and Welch WR (1983). Determinants of ovarian cancer risk. II. Inferences regarding pathogenesis. *J Natl Cancer Inst* **71**, 717–721.

[30] Levanon K, Crum C, and Drapkin R (2008). New insights into the pathogenesis of serous ovarian cancer and its clinical impact. *J Clin Oncol* **26**, 5284–5293.

[31] Dubeau L (2008). The cell of origin of ovarian epithelial tumours. *Lancet Oncol* **9**, 1191–1197.

[32] Carswell EA, Old LJ, Kassel RL, Green S, Fiore N, and Williamson B (1975). An endotoxin-induced serum factor that causes necrosis of tumors. *Proc Natl Acad Sci USA* **72**, 3666–3670.

[33] Old LJ (1985). Tumor necrosis factor (TNF). *Science* **230**, 630–632.
[34] Balkwill F (2002). Tumor necrosis factor or tumor promoting factor? *Cytokine Growth Factor Rev* **13**, 135–141.
[35] Szlosarek PW and Balkwill FR (2003). Tumour necrosis factor alpha: a potential target for the therapy of solid tumours. *Lancet Oncol* **4**, 565–573.
[36] Szlosarek P, Charles KA, and Balkwill FR (2006). Tumour necrosis factor-alpha as a tumour promoter. *Eur J Cancer* **42**, 745–750.
[37] Balkwill F (2006). TNF-alpha in promotion and progression of cancer. *Cancer Metastasis Rev* **25**, 409–416.
[38] Komori A, Yatsunami J, Suganuma M, Okabe S, Abe S, Sakai A, Sasaki K, and Fujiki H (1993). Tumor necrosis factor acts as a tumor promoter in BALB/3T3 cell transformation. *Cancer Res* **53**, 1982–1985.
[39] Moore RJ, Owens DM, Stamp G, Arnott C, Burke F, East N, Holdsworth H, Turner L, Rollins B, Pasparakis M, et al. (1999). Mice deficient in tumor necrosis factor-alpha are resistant to skin carcinogenesis. *Nat Med* **5**, 828–831.
[40] Suganuma M, Okabe S, Marino MW, Sakai A, Sueoka E, and Fujiki H (1999). Essential role of tumor necrosis factor alpha (TNF-alpha) in tumor promotion as revealed by TNF-alpha–deficient mice. *Cancer Res* **59**, 4516–4518.
[41] Scott KA, Moore RJ, Arnott CH, East N, Thompson RG, Scallon BJ, Shealy DJ, and Balkwill FR (2003). An anti–tumor necrosis factor-alpha antibody inhibits the development of experimental skin tumors. *Mol Cancer Ther* **2**, 445–451.
[42] Babbar N and Casero RA Jr (2006). Tumor necrosis factor-alpha increases reactive oxygen species by inducing spermine oxidase in human lung epithelial cells: a potential mechanism for inflammation-induced carcinogenesis. *Cancer Res* **66**, 11125–11130.
[43] Yan B, Wang H, Rabbani ZN, Zhao Y, Li W, Yuan Y, Li F, Dewhirst MW, and Li CY (2006). Tumor necrosis factor-alpha is a potent endogenous mutagen that promotes cellular transformation. *Cancer Res* **66**, 11565–11570.
[44] Bates RC and Mercurio AM (2003). Tumor necrosis factor-alpha stimulates the epithelial-to-mesenchymal transition of human colonic organoids. *Mol Biol Cell* **14**, 1790–1800.
[45] Montesano R, Soulie P, Eble JA, and Carrozzino F (2005). Tumour necrosis factor alpha confers an invasive, transformed phenotype on mammary epithelial cells. *J Cell Sci* **118**, 3487–3500.
[46] Malik ST, Naylor MS, East N, Oliff A, and Balkwill FR (1990). Cells secreting tumour necrosis factor show enhanced metastasis in nude mice. *Eur J Cancer* **26**, 1031–1034.
[47] Orosz P, Echtenacher B, Falk W, Ruschoff J, Weber D, and Mannel DN (1993). Enhancement of experimental metastasis by tumor necrosis factor. *J Exp Med* **177**, 1391–1398.
[48] Orosz P, Kruger A, Hubbe M, Ruschoff J, Von Hoegen P, and Mannel DN (1995). Promotion of experimental liver metastasis by tumor necrosis factor. *Int J Cancer* **60**, 867–871.
[49] Egberts JH, Cloosters V, Noack A, Schniewind B, Thon L, Klose S, Kettler B, von Forstner C, Kneitz C, Tepel J, et al. (2008). Anti–tumor necrosis factor therapy inhibits pancreatic tumor growth and metastasis. *Cancer Res* **68**, 1443–1450.
[50] Naylor MS, Stamp GW, Foulkes WD, Eccles D, and Balkwill FR (1993). Tumor necrosis factor and its receptors in human ovarian cancer. Potential role in disease progression. *J Clin Invest* **91**, 2194–2206.
[51] Wu S, Rodabaugh K, Martinez-Maza O, Watson JM, Silberstein DS, Boyer CM, Peters WP, Weinberg JB, Berek JS, and Bast RC Jr (1992). Stimulation of ovarian tumor cell proliferation with monocyte products including interleukin-1, interleukin-6, and tumor necrosis factor-alpha. *Am J Obstet Gynecol* **166**, 997–1007.
[52] Marth C, Zeimet AG, Herold M, Brumm C, Windbichler G, Muller-Holzner E, Offner F, Feichtinger H, Zwierzina H, and Daxenbichler G (1996). Different effects of interferons, interleukin-1beta and tumor necrosis factor-alpha in normal (OSE) and malignant human ovarian epithelial cells. *Int J Cancer* **67**, 826–830.
[53] Eisen T, Boshoff C, Mak I, Sapunar F, Vaughan MM, Pyle L, Johnston SR, Ahern R, Smith IE, and Gore ME (2000). Continuous low dose thalidomide: a phase II study in advanced melanoma, renal cell, ovarian and breast cancer. *Br J Cancer* **82**, 812–817.
[54] Madhusudan S, Muthuramalingam SR, Braybrooke JP, Wilner S, Kaur K, Han C, Hoare S, Balkwill F, and Ganesan TS (2005). Study of etanercept, a tumor necrosis factor-alpha inhibitor, in recurrent ovarian cancer. *J Clin Oncol* **23**, 5950–5959.
[55] Acosta JC, O'Loghlen A, Banito A, Guijarro MV, Augert A, Raguz S, Fumagalli M, Da Costa M, Brown C, Popov N, et al. (2008). Chemokine signaling via the CXCR2 receptor reinforces senescence. *Cell* **133**, 1006–1018.
[56] Scully RE (1977). Ovarian tumors. A review. *Am J Pathol* **87**, 686–720.